

Development of Thermal Residual Stresses in Film Insert Molding

Hwa jin Oh^a, Jae Ryoun Youn^b

^a Department of Materials Science and Engineering, Seoul National University, Seoul, 151-742

^b Department of Materials Science and Engineering, Seoul National University, Seoul, 151-742

Abstract

Thermal residual stresses are generated in injection molded parts due to non-uniform temperature distribution in the cavity during filling, packing and cooling. Thermally induced residual stresses are studied for a thin plate that is produced by film insert molding(FIM). A thin film is attached on the cavity wall and the resin is injected into the thin plate-like cavity. Development of residual stresses in the film insert molding is modeled and predicted. Thermal history of the part is calculated in the cavity by using a finite difference method to determine the boundary conditions for the flow and residual stress analyses. The moment of the film inserted part is calculated and measured.

Keywords: film inserted molding(FIM), thermal residual stress, finite difference method(FDM), Bending moment

1. Introduction

Film Insert Molding (FIM), also known as In Mold Decorating (IMD) is a new, highly advanced method offering particular benefits to designers, processors and manufacturers of a wide range of products. Compared with traditional methods of product decoration and manufacture, the FIM process offers a number of important benefits; cost effective, durable long life, wide spectrum of formability, and create custom textures. The FIM process, however, is more complex polymer process because of taking into account the influence of an asymmetric cooling method, the re-melting of film parts, and so forth.

In a general case the residual stress in an injected molded part could comprise a number of contributions, including thermal residual stress, packing stress, and flow-induced residual stress. Thermal residual stresses from as a consequence of the thermal gradients that are present during solidification [1-3]. The magnitude of the thermal residual stresses depends on the molding conditions, in particular on the surface temperature of the moldings during solidification [4-5]. Packing stress, resulting from the high pressures imposed during packing, affects the final length shrinkage of a molded product [6]. Flow-induced residual stress, generated as a result of shear, normal and extensional flows during processing, includes anisotropy of several properties, because of the different orientations in the direction parallel and perpendicular to the flow direction[1,3]. Even though there are complex residual stresses in an injected molded part, thermal residual stress, for most polymers of interest, influences mainly the contribution of residual stress field. Hence, the model in this article will only consider thermal induced residual stresses that form in film insert-molded injected parts.

An asymmetric mold wall temperature distribution will cause asymmetric residual stresses; and if the part is not stiff enough, it will warp after its ejection from the mold [7-8]. Although a symmetric mold wall temperature is applied, the thermally induced-residual stress will be asymmetric in the FIM process, respectively. Figure 1 schematically illustrates the

solidification stage of a “plate-like” FIM part. The heat transfer velocity through the thickness at the part 1 differs from the other. Therefore, the residual stress field across the thickness of parts is asymmetric and the thermal bending moment warps the final part. In the first instance, a description of the mechanisms that lead to a thermally induced residual stress is provided and the governing equations of a model for the FIM part are outlined. In a complete treatment, the model requires the coupled solution of a solidification heat transfer and stress equilibrium equation. In this paper the solution from energy equation to thermal moment equation is calculated with the finite difference method to study the influence from the mold temperature difference and Biot numbers.

2. A Thermal-Elastic Residual Stress Model

The thermal-elastic residual stress model presented in this article closely follows and modifies the work of Osswald and Menges[9]. Since mold temperatures are asymmetric in the FIM process, we separate and solve the parts as shown figure 1.

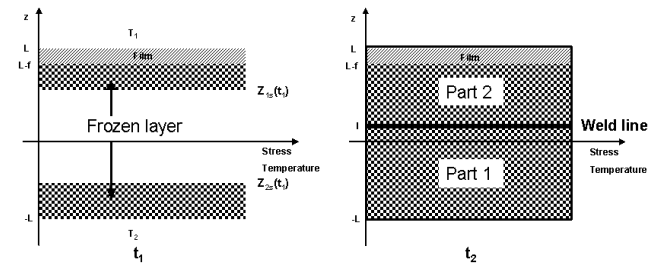


Fig. 1. Schematic of solidification of a film insert molded plate.

2.1 Basic assumptions

For a FIM part with in-plane dimensions that are much larger than the thickness dimension, and with deformation constraint of the FIM part, the major assumptions are as follows:

1) The polymer is amorphous and a liquid region that is

strainfree and stressfree.

2) As the part is thin, the major component of heat transfer during cooling stage is in the thickness direction, heat transfer in the other directions being ignored.

3) A thin layer undergoing solidification at temperature T_g .

This layer undergoes volume contraction and flow resulting in a "flow strain," ε_v , which can also be referred to as a "viscous strain." It is assumed that this strain occurs under hydrostatic stress and is frozen in to the solid layer and, hence, is a function of space alone.

4) A full solid region in the resin part, a thermal strain, $\varepsilon_{th} = \beta(T(z, t) - T_g)$, is formed, where β is the thermal expansion coefficient.

5) Bending is taken into account only after the product is ejected from the mold.

6) The continuity of the temperature and the heat flux is applied at the interface between the film and the resin part.

7) There is no residual stress in the film part.

2.2 A thermal-elastic residual stress model

Under the assumption that the total strains in the part 1 and part 2, $\varepsilon_1(t)$ and $\varepsilon_2(t)$, are, at a given instant in time, uniform across the plate thickness these observations lead to the expression for the total strains as a function of time

$$\begin{cases} \varepsilon_1(t) = \varepsilon_e(z, t) + \beta(T(z, t) - T_g) + \varepsilon_v(z) & (\text{at } -L \leq z \leq I) \\ \varepsilon_2(t) = \varepsilon_e(z, t) + \beta(T(z, t) - T_g) + \varepsilon_v(z) & (\text{at } I \leq z \leq L - f) \end{cases} \quad (1)$$

where ε_e is the elastic strain. In order to make forward progress from Eq. (1) a method for evaluation of the flow strain, $\varepsilon_v(z)$, is required. From Hooke's Law, assuming that Poisson's ratio and Young's modulus are constants, the stress in the frozen layer, is given by

$$\sigma(z, t) = \frac{E}{1 - \nu} [\varepsilon(t) - \beta(T(z, t) - T_g) - \varepsilon_v(z)] \quad (2)$$

Further, equilibrium requires that the integral

$$\int_{-L}^L \sigma(z, t) dz = 0 \quad (3)$$

Combining Eqs. (2) and (3) gives

$$\begin{cases} \int_{-L}^{z_{1s}} \frac{E}{1 - \nu} [\varepsilon(t) - \beta(T(z, t) - T_g) - \varepsilon_v(z)] dz = 0 & (-L \leq z \leq I) \\ \int_{z_{2s}}^{L-f} \frac{E}{1 - \nu} [\varepsilon(t) - \beta(T(z, t) - T_g) - \varepsilon_v(z)] dz = 0 & (I \leq z \leq L) \end{cases} \quad (4)$$

which upon manipulation and integration of the total strain gives

$$\begin{cases} \varepsilon(t) = \frac{1}{z_{1s} + L} \int_{-L}^{z_{1s}} [\beta(T(z, t) - T_g) + \varepsilon_v(z)] dz & (-L \leq z \leq I) \\ \varepsilon(t) = \frac{1}{L - f - z_{2s}} \int_{z_{2s}}^{L-f} [\beta(T(z, t) - T_g) + \varepsilon_v(z)] dz & (I \leq z \leq L) \end{cases} \quad (5)$$

At the solidification front, $z = z_s$, the thermal and elastic strains are zero; and by Eq. (1), $\varepsilon(t) = \varepsilon_v(z)$, which means that Eq. (5) can be written as

$$\begin{cases} \varepsilon_v(z_{1s}) = \frac{1}{z_{1s} + L} \int_{-L}^{z_{1s}} [\beta(T(z, t) - T_g) + \varepsilon_v(z)] dz & (-L \leq z \leq I) \\ \varepsilon_v(z_{1s}) = \frac{1}{L - f - z_{2s}} \int_{z_{2s}}^{L-f} [\beta(T(z, t) - T_g) + \varepsilon_v(z)] dz & (I \leq z \leq L) \end{cases} \quad (6)$$

Assuming no relaxation, this flow strain is frozen in place and will not change. Hence, if information on the evolving transient thermal field, $T(z, t)$, and location of z_s to determine the flow strain profile, $\varepsilon_v(z)$. This calculation needs to be continued up to when the weld surface, $z = I$, becomes solid, at which point the flow strain profile will be fully determined. From the calculated flow strain profile, $\varepsilon_v(z)$, the total strain, and the residual stress distribution, when the plate has cooled to room temperature, T_f , can be found from expressions

$$\begin{cases} \varepsilon_{tot_1} = \frac{1}{I + L} \int_{-L}^I [\beta(T_{f_1} - T_g) + \varepsilon_v(z)] dz & (-L \leq z \leq I) \\ \varepsilon_{tot_2} = \frac{1}{L - f - z_{2s}} \int_{z_{2s}}^{L-f} [\beta(T_{f_2} - T_g) + \varepsilon_v(z)] dz & (I \leq z \leq L) \end{cases} \quad (7)$$

respectively.

2.3 A thermal moment model

Total strain, ε_{tot} , is the entire or actual shrinkage of plate in the change of temperature, Young's modulus, Poisson's ratio and the thermal expansion coefficient. Based on classical shell theory and using the stress distribution, one can additionally compute a thermal moment as follows:

$$M = \frac{E}{1 - \nu} \left[\int_{-L}^I (\varepsilon_{tot_1} - \beta(T_{f_1} - T_g) - \varepsilon_v(z)) \cdot z dz + \int_I^{L-f} (\varepsilon_{tot_2} - \beta(T_{f_2} - T_g) - \varepsilon_v(z)) \cdot z dz \right] \quad (8)$$

This moment will warp the final part and lead to a deflection of the FIM plate.

3. Numerical Solution

The transient temperature field, $T(z, t)$, and location of the solidification front, z_s , needed in Eq. (6) can be determined numerically. For amorphous polymers a model can be based on an enthalpy formulation [10-11].

$$\rho \frac{\partial H}{\partial t} = k \frac{\partial^2 T}{\partial z^2} \quad (9)$$

where the enthalpy $H = c_p T + gL$, L is the latent heat of the polymer. c_p is the specific heat, k the thermal conductivity, ρ the density, and g is the liquid fraction taking a value of zero in the solid and one in the liquid. Upon introducing the dimensionless variables

$$z^* = \frac{z}{b} \quad t^* = \frac{kSt}{\rho c_p b^2} \quad T^* = \frac{T - T_g}{T_s - T_f} \quad (10)$$

$$H^* = St T^* + g \quad St = \frac{c_p (T_s - T_f)}{L} \quad Bi = \frac{hb}{k}$$

where h is the convective heat transfer coefficient at the surface $z = 0$, the governing equation becomes

$$\frac{\partial H^*}{\partial t^*} = \frac{\partial^2 T^*}{\partial z^{*2}} \quad (11)$$

subject to the boundary conditions

$$\left. \frac{\partial T^*}{\partial z^*} \right|_{z=0} = -Bi(T^* + 1) \quad \text{and} \quad \left. \frac{\partial T^*}{\partial z^*} \right|_{z=b} = 0 \quad (12)$$

The key dimensionless groups in the preceding equation are the Stefan number, St ; the ratio of sensible to latent heat, which controls the phase change; and the Biot number, Bi , the ratio of convective heat removal to heat conduction, which controls the cooling.

Equations (11) and (12) can be readily solved using, for example, an explicit enthalpy scheme

$$H_i^{new} = H_i + \frac{\Delta t}{\Delta z^2} [T_{i-1} - 2T_i + T_{i+1}] \quad (13)$$

where i is a node counter on space grid with uniform step Δz ; Δt is a time step; the superscript new refers to values at the new time level; and, for presentation convenience, the $*$ superscript has been dropped. In a given time step the solution of Eq. (13) will provide an updated nodal enthalpy field. The corresponding updated temperature field follows on setting

$$T = \begin{cases} \frac{H-1}{St} & H > 1 \\ 0 & H = 1 \\ \frac{H}{St} & H < 1 \end{cases} \quad (14)$$

The time at which the solidification front reaches node i , that is, $z_s = i\Delta z$, is given when the nodal enthalpy $H_i = 0.5$. At this point the current nodal temperature distribution can be used in a numerical integration of Eq. (6) to obtain a corresponding nodal distribution for $\varepsilon_v(z_i)$. These nodal values can subsequently be used to calculate the residual stress profile through the part thickness.

4. Numerical Results

In variable processing conditions, transient temperature profiles, residual stress profiles and moments are predicted corresponding to the material property data given in Table. 1. And FIM processing condition, applied to numerical simulation, is given in Table 2. In this processes film thickness is a constant, 5 mm in order to neglect effects of change of film thickness. Cooling time should be set for solidification of resin that implies any local temperature decreased under the glass temperature of the resin polymer.

In practical FIM processing the film-side mold wall temperature is controlled near room temperature because the mechanical strength of the film has low resistance to heat. Therefore the film-side temperature is set up as 30, 40, and 50 °C. And then the resin-side mold wall temperature is established to have linear mold temperature differences. The thickness of resin part influences significantly Biot number of plate.

Table 1 Material data

Material Data	Resin	Film	Mold
Young's modulus MPa	2780	2780	-
Poisson's ratio	0.23	0.23	-
Thermal expansion coefficient $^{\circ}C^{-1}$	6.7×10^{-5}	-	-
Heat transfer coefficient $W / m^2^{\circ}C^{-1}$	-	-	2.5×10^4
Thermal conductivity $W / m^{\circ}C$	0.21	0.15	29
Specific gravity kg / m^3	1.13	1.05	7.8
Heat capacity $J / kg^{\circ}C$	2.13×10^6	2.082×10^6	4.6×10^5

Table 2 FIM processing condition for numerical simulation

Condition No.	Cooling time sec	Mold temperature difference ΔT $^{\circ}C$	Film-side mold wall temperature T_2 $^{\circ}C$	Thickness of resin part mm
1	15	10, 20, 30, 40	30	2.5
2	15	0, 10, 20	40, 50	2.5
3	20	0, 10, 20	30, 40, 50	3.5

In interpreting the stress distribution at condition 1 in Fig. 2, it is important to note that, due to the requirement that stresses be in equilibrium, the area under a residual stress curve needs to be zero. A given curve represents a balance between compressive stresses at the part surface and tensile stresses at the part center. Although the residual stress curves are typically parabolic in shape, this results in curves, representing different mold wall temperature differences, show asymmetric curvatures, crossing over each other at about the same point.

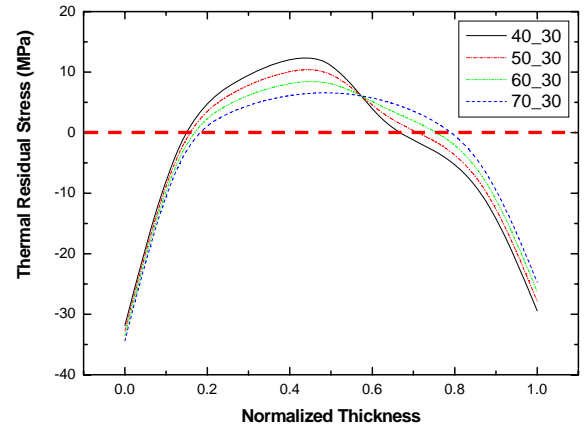


Fig. 2. Residual stress distribution at four different mold temperature differences

The moment of part varies linearly with respect to mold temperature differences in Figure 3. Since resin-side mold wall temperature only is changed in each numerical analysis, this curve implies that the moment of part is in proportion to it.

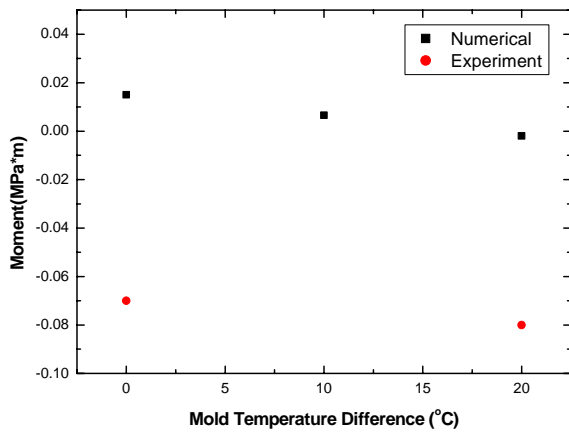


Fig. 3. Moment of plate with increasing the mold wall temperature difference

Figure 4 shows the Biot number of resin part more influences moment of plate per mold temperature difference than one of film part. Biot number involving effect of the thickness of a part and thermal properties is a big deal of weight on warpage of FIM parts. The film part has a smaller one in the whole part that it does not have sensitive effect on the part. And Biot number of a resin part influence warpage of FIM parts significantly.

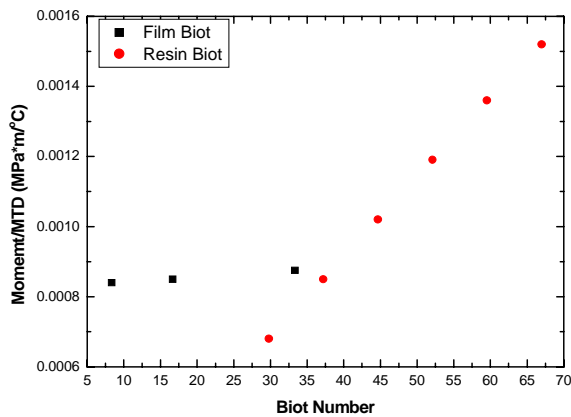


Fig. 4. Moment of plate per mold temperature difference with respect to

5. Experimental Results

In this section, results of the calculations are compared with experimental results for two different test condition specimens. Specimen (a) and (b), shown in Figure 5., are molded of PC/ABS (polycarbonate/acrylonitrile-butadiene-styrene) alloy (staroy PC/ABS HP-1000X) at the Samsung Cheil industry. Film attached on a mold wall is a mirror surface film for insertion molding and for heat molding to witch complex processes at Shin-Etsu polymer. The main processing parameters are summarized in Table 3.

Table 3 FIM processing condition for experiment

Condition No.	Cooling time sec	Mold temperature difference ΔT °C	Film-side mold wall temperature T_2 °C	Thickness of resin part mm
1	30	0	43	3.5
2	35	20	43	3.5

Figure 5 shows deflection and warpage of two specimens molded within two different conditions. In Figure 5 (a), even though symmetric mold wall temperature is set on processing, variation in the cooling rate from the mold wall to its center due to film on the one-side wall causes asymmetrical thermal-induced residual stress. Such unbalanced cooling rate results in an asymmetric tension-compression pattern across the FIM part, causing a bending moment that tends to cause part warpage. In Figure 5 (b), although asymmetric mold wall temperature is applied to the processing, deflection of the part decreased comparing with specimen (a). It is noted in Figure 3. Moment of the part decreases as the mold temperature difference increases. But experimental data for moment of the part is under-estimated than calculations. There are three different schematic residual stresses in an actual molded part. However calculations consider only the thermal-induced residual stress.

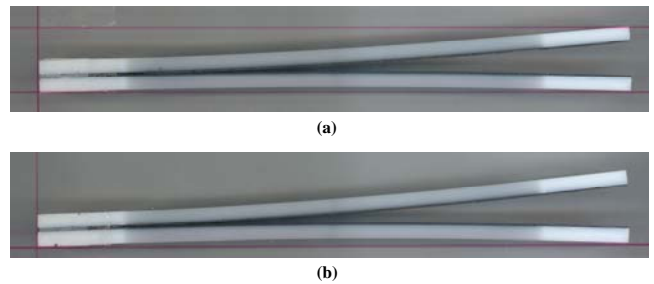


Fig. 5. Warpage of the polycarbonate/acrylonitrile-butadiene-styrene alloy plate using the image processing technique; (a) condition 1, (b) condition 2.

6. Conclusion

In this study, thermal-induced residual stresses in FIM molded parts were predicted by numerical simulation and also moment of the parts was calculated and compared with experiments.

Although many effects contribute to residual stresses during FIM processing of polymers (e.g., packing pressure, viscoelastic relaxation, nonconstant material properties), its formation may be adequately modeled using a one-dimensional thermoelastic treatment that assumes constant material properties. This model requires the coupled solution of thermal solidification problem and evaluation of the integral of stress through the part thickness. In this article it has been calculated completely.

Thermal-induced residual stress distribution depends remarkably on Biot number as shown in Figure 5. With a large Biot number, heat is rapidly removed through the surface, resulting in absolutely high residual stresses. And unbalanced cooling rate causes asymmetrical residual stress distribution.

Moment of the part was linearly increasing with respect to mold temperature difference because the thermal strain mainly affects the total strain.

Part warpage results from molded-in residual stresses, which is caused by differential shrinkage of material in the molded part. Non-uniform cooling rate through the part surface induces different shrinkage. The material cools and shrinks inconsistently from the mold wall to the center, causing warpage ejection. In FIM part, increasing mold temperature difference causes decreasing warpage of the part, compared to increasing in general injection molded parts. Therefore a study may be done to understand the effect of the substrate, the film on the one side wall, as well as asymmetric temperature boundary condition for

the thermal-induced residual stresses.

Acknowledgements

This study was financially supported by the Korea Science and Engineering Foundation through the Applied Rheology Center (ARC) at Korea University.

References

- [1] B. Haworth ; C. S. Hindle ; G. J. Sandilands ; and J. R. White, *Plast. Rubb. Proc. Appls.* 1982, 2, 59
- [2] J. R. White, *Polym. Test.* 1984, 4, 165. Also appeared as Ch. 8 in *Measurement Techniques for Polymeric Solids* R. P. Brown & B.E. Read, eds., Elsevier Appl. Sci. Publs., Barking, U.K. 1984.
- [3] A. I. Isayev; and D. L. Crouthamel; *Polym. Plast., Technol. Eng.*, 1984, 22, 177
- [4] A. Siegmann; A. buchman; S. Kenig, *Polym. Eng. Sci.*, 1982, 22, 561.
- [5] R. F. Eduliee; J. W. Gillespie, Jr.; R. L. McCullough; *J. Thermoplast. Compos. Mater.*, 1989, 2, 320.
- [6] K. M. B. Jansen; G. Titomanlio, *Polym. Eng. Sci.*, 1996, 36, 2029.
- [7] O. Denizart; M. Vincent; J. F. Agassant, *J. Mater. Sci.*, 1995, 30, 552.
- [8] H. H. Chiang; K. Himasekhar; N. Santhanam; K. K. Wang, *J. Eng. Mater. Tech.*, 1993, 115, 37.
- [9] T. A. Osswald; G. Menges, *Material Science of Polymers for Engineers*, Hanser, Munich, 1996.
- [10] V. R. Voller, *Adv. In Numer. Heat Transfer*, 1996, 1, 341-375.
- [11] B. A. Boley and J. H. Weiner, *Theory of Thermal Stresses*, Dover, 1960.